

See discussions, stats, and author profiles for this publication at: <https://www.researchgate.net/publication/358166774>

Artificial neural networks controller of active suspension for ambulance based on ISO standards

Article in *Proceedings of the Institution of Mechanical Engineers Part D Journal of Automobile Engineering* · January 2023

DOI: 10.1177/09544070221075456

CITATIONS

10

READS

224

2 authors:



Anis Hamza

Université de Tunis

763 PUBLICATIONS 139 CITATIONS

[SEE PROFILE](#)



Noureddine Ben Yahia

ENSIT

73 PUBLICATIONS 184 CITATIONS

[SEE PROFILE](#)

Some of the authors of this publication are also working on these related projects:




Optimization and modeling of CAPP by Hybrid approach [View project](#)



Personnel Certification [View project](#)

Artificial neural networks controller of active suspension for ambulance based on ISO standards

Proc IMechE Part D:
J Automobile Engineering
2023, Vol. 237(1) 34–47
© IMechE 2022
Article reuse guidelines:
sagepub.com/journals-permissions
DOI: 10.1177/09544070221075456
journals.sagepub.com/home/pid


Anis Hamza¹ and Nouredine Ben Yahia

Abstract

The level of vibration to which a patient is subjected in an ambulance is often too high. Ambulance personnel should take steps to reduce these vibrations. To avoid slowdowns and other barriers that create high vibration peaks, the speed is reduced or the ambulance deviates from the quicker or shorter path. This work implements Artificial Neural Network (ANN) control over five low-cost active shock absorbers proposed to decreasing the impact of vibration on a patient's body during an ambulance ride. For this, the passive shock absorber is replaced by a new actuator consisting of a conventional hydraulic cylinder with a proportional butterfly valve placed outside the cylinder between its orifices. The ANN is used to adjust the damping coefficient. The ANN controller inputs are the accelerations of the sprung and unsprung masses, and the output is the valve opening area. Two forces may be exerted by this active suspension system: one is used to compensate for the mass of the stretcher, the patient and the medical equipment if present and a second is used to actively isolate the patient from the vibrations of the ambulance. The performance of the active suspension ambulance is contrasted to that of a traditional ambulance, in which the stretcher is rigidly linked to the ambulance body. When compared to alternative controllers, the findings showed that the proposed register controlled by ANN performed better. The simulations demonstrate that the active system may minimize the vibrations of the patient's mass and the stretcher by more than 70% for random abnormalities in the road that meet the ISO2631-5 and ISO 8608 standards.

Keywords

Ambulance, stretchers, active suspension system (ASS), vibration, artificial neural networks (ANN)

Date received: 7 June 2021; accepted: 4 January 2022

Introduction

Driving comfort and good handling of the vehicle are the main functions of the vehicle's suspension system. Designers of suspension systems generally aim to achieve these goals while keeping cost and energy consumption minimal. Each type of suspension system is characterized by the type of shock absorber¹ and each has its own advantages and disadvantages. Passive suspension, which is equipped with a passive shock absorber, is most often installed in almost all types of vehicles. Its low cost and simple construction make it the most economical option for all car manufacturers. In addition, it enjoys a reasonable level of vehicle suspension performance.² The problem with such a system is that it has a constant damping coefficient. As a result, passive suspension systems are unable to adapt to changes in the vehicle's condition, which might be induced by a change in road type or even a shift in the vehicle's weight distribution. As a result, the performance of a vehicle with a standard suspension system

can only be altered by replacing the shock absorber with one that has a different damping coefficient.³

Rather, active suspension uses a hydraulic/pneumatic circuit that includes a linear actuator.⁴ The system is also equipped with road prediction sensors that can read the profile of the road ahead of the vehicle. This combination works together so that the actuator keeps the vehicle at a stable vertical level and completely isolates the vehicle from road vibrations. However, there are many issues with active suspension systems such as heavy electrical consumption that requires a considerable portion of engine power to

Mechanical, Production and Energy Laboratory (LMPE), National School of Engineering of Tunis (ENSIT), University of Tunis, Tunis, Tunisia

Corresponding author:

Anis Hamza, National School of Engineering of Tunis (ENSIT), Mechanical, Production and Energy Laboratory (LMPE), Avenue Taha Hussein Montfleury, University of Tunis, Tunis 1008, Tunisia.
Email: anis7amza@gmail.com

drive the hydraulic components. It also has a rather high weight, which adds to the vehicle's total weight. In addition, Active suspension is characterized by the need for an external source of energy. This energy triggers the control mechanism, which regulates the force produced by the suspension system on a constant basis. Very often, the control system reacts to vehicle parameters (speeds and movements). These active suspension systems are in fact systems in which the springs and shock absorbers are replaced partially or totally by actuators. The latter's force is generated in accordance with, of course, in accordance with a control law that utilizes the data from the numerous sensors attached to the vehicle. These sensors can include accelerometers, displacement sensors which can provide information, for example, on the deflection of the suspension, gyroscopes, etc.

When a person becomes ill unexpectedly or suffers more serious injuries in an accident, they must be transferred swiftly and safely to a facility where they may receive proper treatment. In these instances, the vehicles are heavier and less comfortable than passenger automobiles. Around the world, ambulances have generally been customized or adapted from heavy transport vehicles, such as trucks or vans (See Figure 1). Because patients are transported in the back of the vehicle, they are subjected to accelerations during transportation, which are caused by brakes, turns, crossing barriers, or uneven pavements, all of which have a direct impact on the vehicle's movements.⁵

Literature review

Ambulances are important in transporting injured patients yet as providing aid to patients. The shaking and instability of the ambulance easily can result in nausea, deterioration of the patient's condition and also the possibility of death.⁶ Patients are especially sensitive to the insignificant intensity of vibration.

When the ambulances are in operation, the vibrations in the lateral direction, due to the bends, would make emergency care difficult for the paramedic to operate and even cause trauma for the patient. In addition, the subsequent pitching motion due to frequent braking and starting will generate negative acceleration from the feet to the head in the patient, which will lead to side effects, such as rapid movement of blood to the head,⁷ reduction venous return and increased blood pressure in the patient.

In order to attenuate these vibrations for lying patients, studies have focused on the stretcher suspension system and the vehicle body suspension system. So far, a limited number of studies have been conducted for the stretcher suspension system, involving passive, semi-active, and active techniques.

For example, Henderson and Raine⁸ studied a semi-active air suspension for stretcher. Sagawa et al.⁹ conducted research into the quality of driving an actively



Figure 1. Transportation for critically patients.

controlled stretcher system to improve the blood pressure variation of the lying patient. These studies, for semi-active and active suspension systems, have focused on attenuating the vibrations of patients on the stretcher and did not address the issue of vibration and stability from the perspective of paramedics.

Another way to improve the ride quality of the patient is to design a suspension system specific to the vehicle body. The advanced suspension system will improve ride comfort and ride stability for reclining patients and paramedics.

Usually, ambulances are conventionally converted from a truck or van. Their passive suspensions, although adequate for the original vehicle, are unable to meet the demands of ambulance driving. Cao et al.¹⁰ studied the dynamic characteristics of the hydro-pneumatic suspension interconnected to the pitch, which indicated that the proposed suspension could offer significant advantages to improve both handling and driving qualities. Zhang et al.¹¹ proposed a hydraulically interconnected (HIS) roll/pitch plane suspension to improve roll/pitch resistance performance without sacrificing ride comfort.

Xu et al.¹² optimized the damping characteristic of stretchers on emergency ambulances. Pan and Zhang¹³ also studied the vibration isolation performance of the ambulance stretcher. Yang et al.^{14,15} demonstrated a nonlinear vibration reduction stretcher system for a tracked ambulance. Prehn et al.¹⁶ investigated vibration and noise levels during infant transport and provided reliable means of improvement. Chae and Choi¹⁷ have proposed a vibration isolation bed stage with magnetorheological dampers, which can control the vibrations in the stretcher as well as the vibrations of the seat for the paramedic. The drawbacks of this vibration isolation system, such as structural complexity and operational drawbacks, limit its application. In fact, the structure of the simple stretcher without a suspension system is still very popular in practical applications due to its convenient operation while transporting the patient. Ding et al.¹⁸ proposed a rolling resistant HIS for three-axle straight trucks, and a design methodology for the parameters of the HIS was also presented. Yang et al.¹⁹ introduced a kinetic dynamic suspension system that can improve handling and handling. Tan et al.²⁰ offers

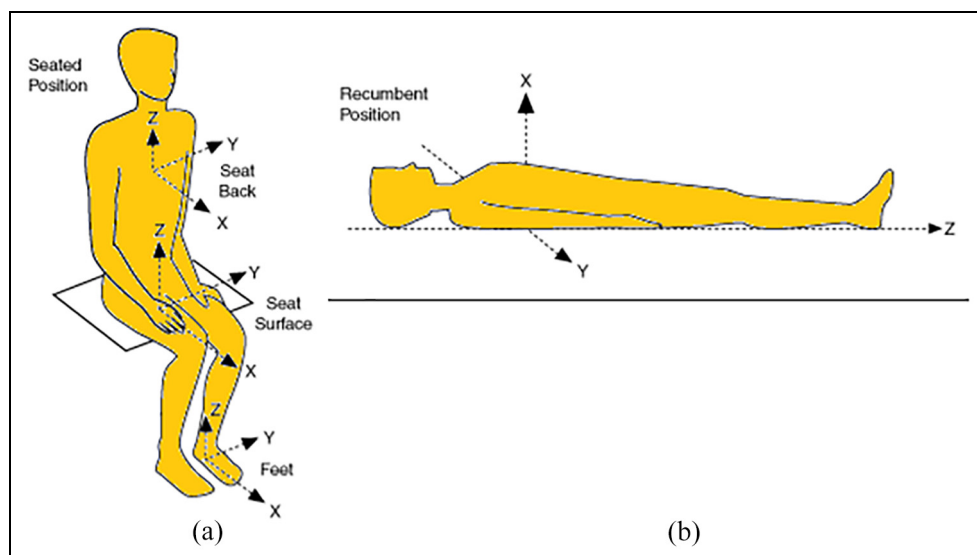


Figure 2. Coordinate system for the various contact points of entry for vibration of ambulance occupants when subjects are in: (a) a seated position and (b) a recumbent position.

an interconnected hydro-pneumatic pitch-roll suspension system that can achieve resistance control for ambulance pitch, roll, and rebound modes to improve stability and dampen vibrations for lying patients.

Standards for Emergency Medical Transport

The standard patient care policy is to require by Emergency Medical Assistance Services (EMAS) ambulance teams to conduct the minimum necessary treatment on site to stabilize the patient as quickly as possible. Since January 1, 2021, all land medical transport vehicles must comply with standard EN 1789²¹ and EN 1865²² for compulsory ambulance equipment. From January 1, 2021, new vehicles must meet standard EN 1789 and EN 1865 for compulsory ambulance equipment. It establishes the minimum design and performance standards for equipment used to carry patients in ambulances. This European Standard applies to road ambulances that can carry at least one passenger on a stretcher. Therefore, a great deal of basic, intermediate and advanced rescue procedures must be performed in the mobile ambulance. This ensures rapid transportation to the acute care facility. Critically ill patients should be transported in no more than 10 min, while other patients or trauma patients should be transported in no more than 20 min, according to the treatment standards. As our society becomes more litigating and damage lawsuits increase against the emergency medical services, the safety of occupants in intensive care vehicles has become a major concern. Given the health of most ambulance patients already at risk and the relatively limited and limited healthcare environment of a moving vehicle, the risk of injury or death from adverse events occurring during emergency transport is high enough to warrant a study.

In this study, driving comfort will be assessed using the ISO 2631-5 standard. The standard evaluation of human exposure to whole body vibration in terms of mechanical vibration and shock scope is ISO 2631-5.²³ As this study only looks at vertical movement, the entire assessment of ride comfort is done on W_k (Vertical vibration of the whole body along the Z axis: seated or recumbent person as shown in Figure 2(a) and (b) respectively).

The important functions of the human body (cardio-vascular system, skeletal system, central nervous system, respiratory system) can be affected by vibrations from an uneven surface, and a patient's clinical status can deteriorate.²⁴ Patients who have had a heart attack or stroke, or who have impairments that cause persistent pain and discomfort (arthritis, multiple sclerosis, back pain), require extra attention since they are more sensitive to the vibrations created during transportation, which might harm their health.²⁵ The ISO 2631 standard²⁶ explains how to measure the human body's vibration exposure. This standard covers human exposure to numerous mechanical shocks and establishes parameters for multiple shocks measurement. The findings of these measures are then examined to provide information for determining the risk of unfavorable health effects from compression on the vertebral endplates of the lumbar spine in sitting persons. Even if the tip plate is not injured, other injuries might occur.²³ When compared to standing or sitting, patients who are moved while lying are more sensitive to vertical vibrations.^{27,28} Furthermore, for the sick or injured, the vibrations of the human body are the most distressing. The difference in road level might be blurry or even wide depending on which side of the road the ambulance is crossing. Irregularities encountered along the road might take the form of a pocket or a random

profile. Random road roughness is classified by power spectral density (PSD) for both paved and unpaved roads^{29,30} according to ISO 8608.

In light of the foregoing, this article presents a dynamic study of an ambulance that takes into account a variety of operational scenarios, including braking and driving on uneven ground. Since the previous articles, on ride comfort generally does not focus on a specific type of ambulance transport.

The goal of this research is to look at how patients' own motions and acceleration might impact their comfort while being carried in ambulances. The results obtained provide input to the development of a new intelligent system to reduce the effects of vibrations on the patient's body using an active suspension ANN controller device.

The situation and problematic study

The ambulance stretcher is a very simple construction that is used to transport the patient. With the accelerations caused by a quick ambulance trip, this can be a serious trauma for the patient. To compensate for the road profile and accelerations caused by the ambulance's trajectory, a specific active control system was installed between the ambulance frame and the stretcher, as well as a possible control strategy.

The many sources of vibration in patient ground transportation are determined by uneven roads, variable road profiles, and vehicle suspension. The vibration can cause nausea, discomfort, headache, impaired visual performance, pain at the fracture site, worsening of spinal damage and internal brain hemorrhages with interference in intravenous cannulation, endotracheal intubation, etc. These vibration effects can be minimized by using attendant restraints, vibration absorbing mattresses, and padding of vehicle-patient contact points.

For seriously injured patients, transport by ambulance is often very dangerous. During about 28.8% of trips,^{31,32} some deterioration of the patient occurs. In order to prevent this hazard, the ambulance's speed must frequently be reduced significantly, yet this is plainly perilous.

A comprehensive multi-body vehicle model was utilized to analyze the patient's body exposure to vibration during ambulance travel. The tipper trucks are non-linear and the flexible suspension effect is also taken into account. The tire's mathematical model is similarly non-linear. The simulation settings correspond to the FIAT DUCATO 2.3 JTD 8M3 ambulance³³ modified to the Intensive Care Unit (ICU) model, which is routinely used to deliver patients to EMAS (See Figure 3).

The deployment of autonomous cars is one of the most recent breakthroughs. Vehicles that have been customized to convey the sick are insufficient.



Figure 3. Ambulance vehicle FIAT DUCATO 2.3 JTD 8M3.

As a result, the design of an ambulance stretcher controller based on artificial neural networks is critical in this context (ANN).

This makes it possible to reduce these inconveniences of these modified vehicles, and to ensure the safe and rapid transport of the patients. The contribution of our paper is to propose a control model of an ambulance to ensure the comfort of patient transport in urgent cases. We have also, verified the validation of this complete model by numerical simulations based on experimental data extracted from other works.

Mathematical formulation

The studies mainly focused on the composition of mathematical algorithms, theoretical calculations, and the influence of various factors on the oscillation characteristics of the vehicle during the process of emergency patient transport. The surveys incorporated numerical and analytical methods. The mathematical models developed allow the movement of vehicles to be determined and facilitate investigations of the effects of vibrations of road profile excitations related to the processes of transporting patients by ambulance.

The most hazardous vibrations for laying patients are between 2 and 8 Hz, which is similar to the human body's natural frequency.³⁴ In this frequency range, vibrations induced by road imperfections and transmitted by car suspensions are fairly severe; using a device to isolate the patient (see Figure 4) can give considerable advantages. Furthermore, the accelerations caused by the ambulance's trajectory (curves and speed fluctuations) are hazardous to patients.

This research is based on simulating an ambulance ground suspension system using a model of an automobile quarter with one degree of freedom in the vertical axis that we constructed before.³⁵ For this reason, the focus was on the vertical vibrations transmitted to the patient's body through the ambulance floor surfaces running along the z axis to better relate the measured

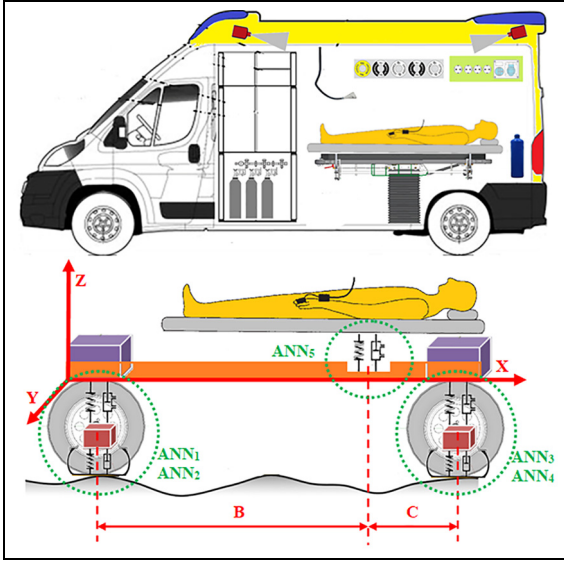


Figure 4. The orientation of measurement axes for simulation and experimental tests.

vibrations to the vehicle model, the effects on health and road excitation.

While it's recognized that longitudinal and transverse accelerations exist within the ambulance compartment, they're often because of rapid starts, rapid decelerations or sharp turns which might be greatly reduced by instruction and training of the motive force. Figure 5 shows a diagram of a system that is used to generate active suspension.³⁶

The dynamic equations of the active suspension system (See Figure 5) are as follows:

$$\begin{cases} M_s \ddot{Z}_s + \eta_s (\dot{Z}_s - \dot{Z}_u) + (F_s - F_a) = 0 \\ M_u \ddot{Z}_u - \eta_s (\dot{Z}_s - \dot{Z}_u) - k_t (Z_r - Z_u) - (F_s - F_a) = 0 \end{cases} \quad (1)$$

Where M_s and M_u are representing the sprung mass and the unsprung mass respectively, Z_r is the road surface position variation, Z_s and Z_u are measured variables representing the sprung mass displacement and the displacement of tire axis (Unsprung mass), respectively. F_s , F_a , and F_f are the nonlinear spring force, the hydraulic actuating force and the hydraulic friction force, respectively.

By taking the Laplace Transform the dynamic equation (1) has been converted to p -domain specifications. The transfer function $G_s(p)$ and $G_u(p)$ representing the sprung mass displacement and the displacement of tire axis, respectively and give an idea about dynamic changes in active suspension system. The variable C and D are control effort and disturbance signal respectively.

When consider the control input, $C(p)$ and the road disturbance, $D(p) = 0$. Thus the transfer function $G_s(p)$ has been arrived:

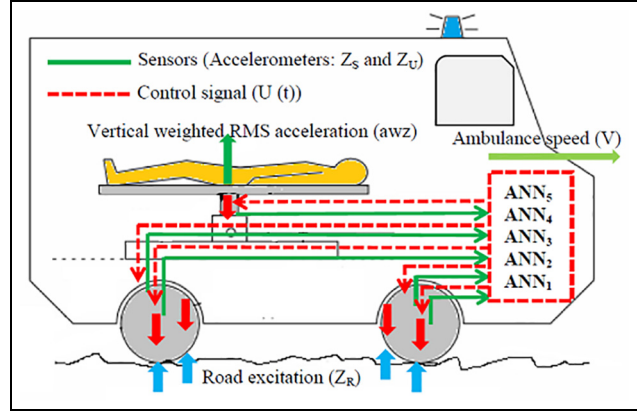


Figure 5. Implementation of these ANN controllers for the ambulance active suspension.

$$G_s(p) = \frac{Z_s(p) - Z_u(p)}{C(p)} = \frac{(M_s + M_u)p^2 + \eta_s p + k_t}{\Delta} \quad (2)$$

If only the disturbance input $D(p)$ considered, then the control input $C(p) = 0$. Thus the transfer function $G_u(p)$ has been arrived.

$$G_u(p) = \frac{Z_s(p) - Z_u(p)}{D(p)} = \frac{-M_s \eta_s p^3 - M_u k_t p^2}{\Delta} \quad (3)$$

Where,

$$\Delta = (M_s p^2 + \eta_s p + k_s)(M_u p^2 + (\eta_s + \eta_u)p + k_s + k_t) - (\eta_s p + k_s)^2 \quad (4)$$

The equation (2) gives the transfer function model of ambulance with control input $C(t)$ and equation (3) gives the transfer model with disturbance input $D(t)$.

The profile of the road model (Input) adopts filtered white noise²⁵ as follows:

$$\dot{D}(t) = \dot{Z}_r(t) = -2\pi f_0 Z_r(t) + 2\pi \sqrt{GV} \omega(t) \quad (5)$$

Where G is the road irregularities coefficient, f_0 is the lower cutoff frequency, V the vehicle speed and $\omega(t)$ the unit white noise.

The relation between the displacement of the spool valve $X_v(t)$, the load flow $Q(t)$, and the continuity equation of the hydraulic cylinder chamber give:

$$\begin{aligned} Q(t) &= K_g(t)X_v(t) - K_c(t)P(t) = A(\dot{Z}_x(t) - \dot{Z}_u(t)) \\ &+ C_T P(t) + \left(\frac{V_T}{4\beta}\right) \dot{P}(t) \end{aligned} \quad (6)$$

In practical hydraulic actuator operations, the valve displacement $X_v(t)$ can be manipulated by a voltage

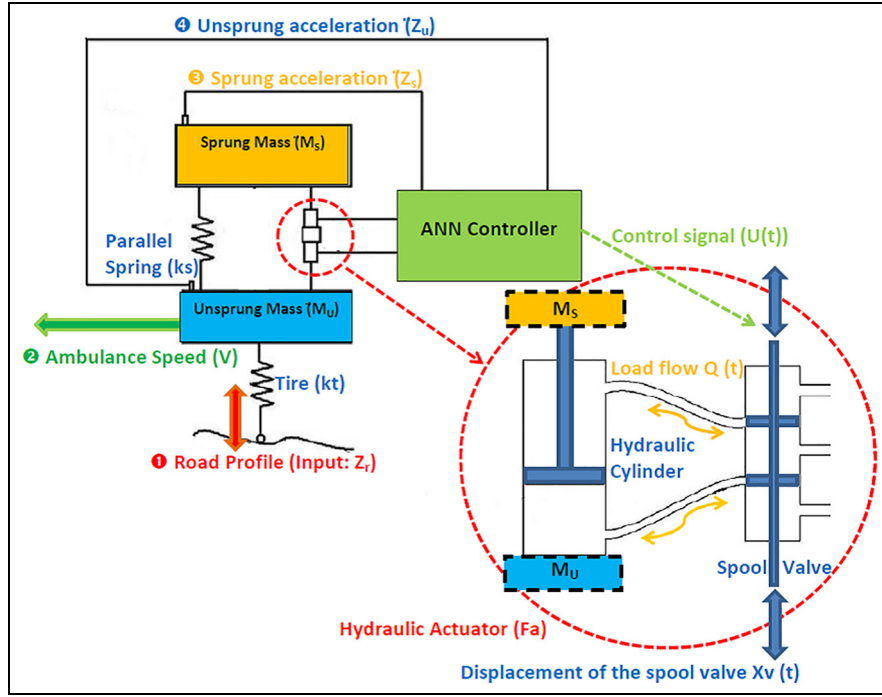


Figure 6. Implementation of ANN Controller of the actuating force of this hydraulic suspension system.

$U(t)$ or current $I(t)$ input in corresponding to different required forces.

This work implements Artificial Neural Network (ANN) control over five low-cost active shock absorbers proposed to decreasing the impact of vibration on a patient's body during an ambulance ride. For this, the passive shock absorber is replaced by a new actuator (See Figure 6) consisting of a conventional hydraulic cylinder with a proportional butterfly valve placed outside the cylinder between its orifices. The ANN is used to adjust the damping coefficient by regulating the opening area of the valve.

The relation between the servo-valve spool displacement and the control voltage described as:

$$X_v(t) = K_v U(t) \quad (7)$$

Then, the time derivative of the actuating force of this hydraulic suspension system derived:

$$\dot{F}_a(t) = A \dot{P}(t) = A \left(\frac{4\beta}{V_T} \right) [K_g(t) K_v U(t) - C_T P(t) - A(\dot{Z}_x(t) - \dot{Z}_u(t))] \quad (8)$$

The dynamic equation of this hydraulic servo control system includes coupling with multiple outputs, time variable, and nonlinear characteristic. It is difficult to estimate these system parameters and use this dynamic equation to design a model-based controller. Therefore, an ANN intelligent control scheme was used to design the active suspension control module. The dynamic

equations for this suspension system have been rewritten as follows:

$$\begin{aligned} M_s V_T \ddot{Z}_s &= -4\beta C_T k_s Z_s - [k_s + 4\beta(C_T \eta_s + A^2)] \\ V_T \dot{Z}_s - (\eta_s + 4\beta C_T M_s) \ddot{Z}_s &+ 4\beta A K_g(t) K_v U(t) \\ &- (4\beta C_T F_f + V_T \dot{F}_f) + \\ [\eta_s V_T \ddot{Z}_u + (k_s V_T + 4\beta A^2 + 4\beta \eta_s C_T) \dot{Z}_u &+ 4\beta C_T k_s Z_u] \end{aligned} \quad (9)$$

Where V_T is the total actuator volume, β is the effective bulk modulus, and C_T is the total piston leakage coefficient.

Model of the proposed ANN

Remember that our problem is to determine the comfort parameters of patient transport from the process inputs. Due to the non-linearity of this problem, a Perceptron Multi-Layer (MLP) is used to predict these parameters (Road profile, Ambulance speed, Ambulance technical characteristics, etc.) for different possible situations and variations in input parameters. Moreover, an MLP can be seen as a black box and therefore the planner can use it in a very simple way without a deep knowledge of its theoretical underpinnings.

The active suspension of an ambulance stretcher may be easily performed by using four parallel controllers for the four wheels, which provide control inputs for an ambulance stretcher controller: fact, the intrinsic

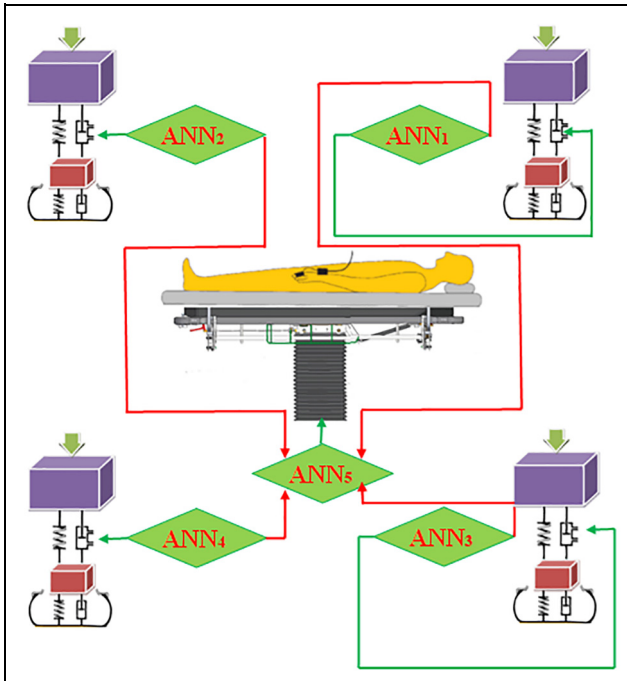


Figure 7. Fully active suspension system for ambulance stretchers.

stiffness and moving masses of the ambulance stretcher make this possible. The limits of a closed-loop drive-train can meet the precision and dynamic performance requirements of this application. A special purpose five

degree of freedom (5 DoF) parallel architecture (See Figure 7) has been proposed.

In Figure 8, the effects of a longitudinal acceleration of an ambulance on the behavior of the system are indicated: if the longitudinal acceleration increases sharply (i.e. with considerable high frequency components of the ambulance position), the first effect sought is an opposite movement of the stretcher in relation to the ambulance.

For the learning phase 5 neural networks are created (ANN_1 , ANN_2 , ANN_3 , ANN_4 , ANN_5) each of them will generate one of the five quality parameters (Road Profile (Input: Z_r), Ambulance speed (V), Sprung acceleration (Z_s), Unsprung acceleration (Z_u), and the nominal ambulance parameters values) as shown in Figures 7 and 8.

In this study, 80% of the randomly selected datasets were went to train the artificial neural networks and therefore the other datasets (20%) were went to test (15%) and verify (5%) the neural networks. Several factors can determine the extent of precision of an ANN like the quantity of hidden layers, the amount of neurons per hidden layer, the quantity of iterations, etc. during this paper, we've considered a "6-n-1" structure for artificial neural networks (from ANN_1 to ANN_5). The quantity of hidden neurons (n) is chosen after numerous simulations to maximize the performance of every network. The basis mean square error and generalization capabilities are considered a benchmark for network performance.

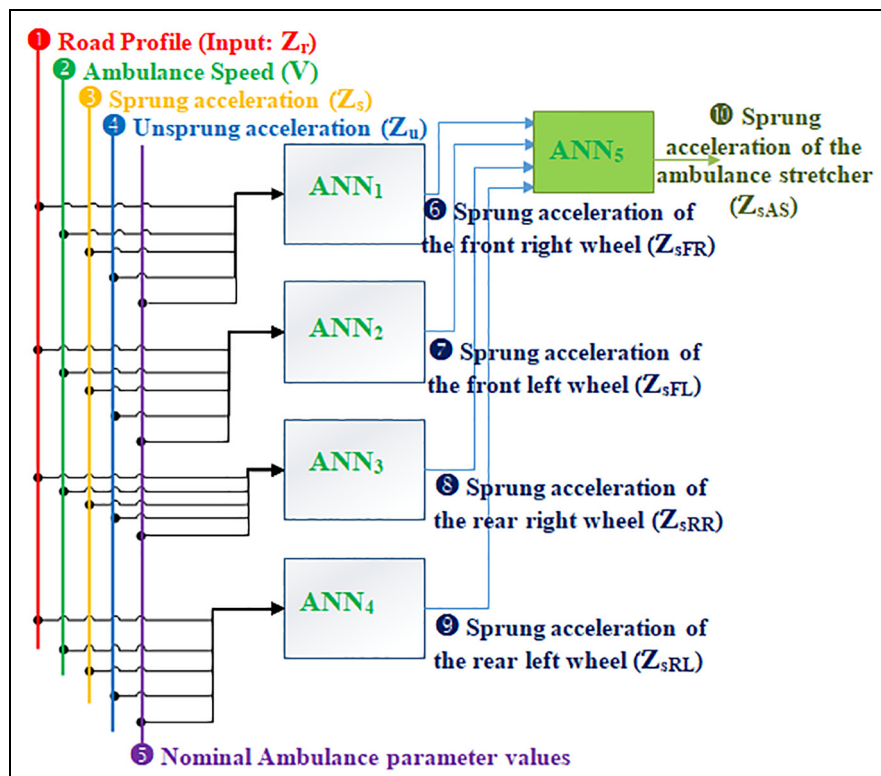


Figure 8. Artificial Neurons Networks architecture.

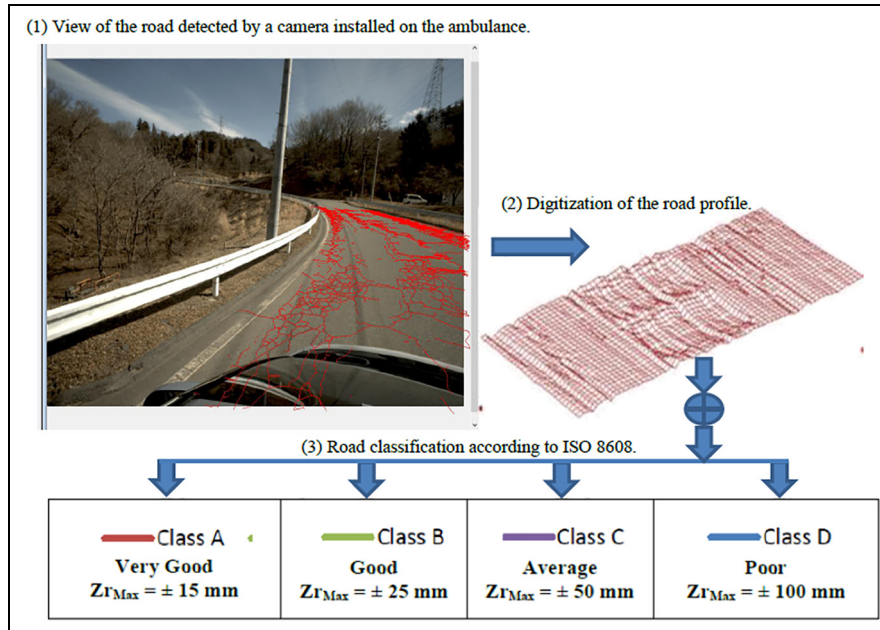


Figure 9. ISO 8608 random road profile classification.

The feed-forward artificial neural networks investigated (from ANN₁ to ANN₅) consist of an input layer, an output layer, and a hidden layer with a configurable number of neurons (See Figure 8). From the input layer to the output layer, information is transferred across layers. The network's response is interpreted from the activation value of its output neurons, including the output vector. At the top of this process, the network should be able to generate the correct solutions for examples that haven't been seen before. This can be the goal of the generalization phase. This process consists in generalizing the network output results for the inputs not belonging to the training base.

It's impossible to predict which learning algorithms will be the most efficient for a specific situation. Many factors influence this, including the difficulty of the problem, the number of input nodes in the training set, the number of weights and polarizations.

Numerical simulation

Numerical simulations will be presented in this part to illustrate the effectiveness of the suggested ANN active suspension control approaches. The technique begins by calculating road profiles corresponding to each roughness class as indicated in Figure 9.

A new method of evaluating driving comfort has been proposed in this article. An interesting new approach to using road measurements to track different levels of excitement is suggested. Finally, it may be interesting to use the measurement data on a route simulator to create algorithms for controlling the ANN active suspensions of ambulances. Before analyzing the parameters of the ambulance (See Table 1), it is

Table 1. Ambulance parameters values used in this study.

Parameter definition	Symbol	Value	Unit
Distance between the front and stretcher axles	B	1.780	m
Distance between the stretcher and rear axles	C	1.325	m
Loaded total mass	M	3.5	Tons
Pitch moment of inertia	I	6.2×10^3	kg m ²
Front axle load capacity	M _F	1.695	Tons
Rear axle load capacity	M _R	1.805	Tons
Sprung mass	M _S	2137	kg
Unsprung mass	M _U	54.3	kg
Elastic stiffness of the sprung mass	K _S	99,760	N/m
Damping coefficient of the sprung mass	η_s	1135	N s/m
Elastic stiffness of the tire	K _T	156,700	N/m
The effective bulk modulus of the system	B	15,500	bar

necessary to understand the different inputs and outputs of the ambulance model.

The changing elevation of the road profile is the input in the instance of the ambulance, while the response to vibration is the output. This vibration, felt by the user, is correlated with perceived comfort.

Figure 9 shows the entry road profiles in the lateral direction at a road parcel length of 250 m. To give an idea of typical classification profiles, examples of simulated profiles with different roughness (Class A, B, C, and D) are presented (See Figure 10). These examples are implemented in accordance with ISO 8608. Driving comfort depends on human perceptions of noise, vibrations, and vehicle movements. Although ride comfort

Table 2. Comfort Scale.

IRI (m/km)		RMS = a_w (m/s ²)	NRMS = a_w/g
9.375	F (Extremely Poor)	2.25	0.229
7	E (Very Poor)	1.4	0.143
4.5	D (Poor)	0.9	0.092
2.75	C (Average)	0.565	0.058
1.625	B (Good)	0.315	0.032
	A (Very Good)		

performance (RCP) differs from person to person, it may be quantified using the approach presented by Abramov et al.,³⁷ and the root mean square (RMS) of the acceleration of the suspended mass normalized by the acceleration of gravity g is determined by equation (1):

$$NRMS = \frac{a_w}{g} = \sqrt{\frac{1}{T} \int_0^T \left[\frac{a_w(t)}{g} \right]^2 dt} \quad (10)$$

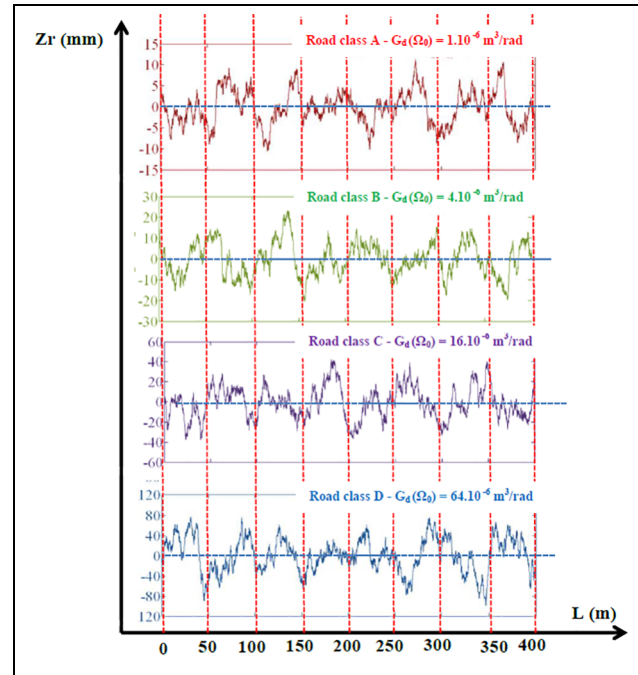
As stated in the introduction to this article, driving comfort depends on many factors. However, ISO 2631–5²⁶ provides approximate guidance on probable responses to total vibration values in public transport. Table 2 shows the different levels of comfort that can appear.

Simulation results and discussion

ANN control of active ambulance

Suspensions. An artificial neural network was implemented in the mathematical model to predict the optimized values using MATLAB's NNTOL Neural Network Toolbox. The Toolbox provides pre-trained algorithms and models to create, train, simulate, and visualize neural networks. The chosen artificial neural network is a look-ahead network in which the unidirectional information comes from the input data to the target data. ANN was implemented in the model in order to predict the optimized configuration parameters. In the end, a comparison between baseline, optimized and predicted values was carried out. The network was implemented in a Quarter Car model, as a first step, in order to predict the parameters capable of reducing the tire deflection and the suspension travel in time domain and frequency domain. This choice was made in order to test the quality of the prediction of the optimal parameters. The designated parameter of the optimization is the depreciation rate.

After having formed the network with a simple Quarter Car model, it is possible to extend the same procedure to the 5-DOF model (We have simplified the study by the assumption that we assume that the angular movements are negligible and the only ones possible

**Figure 10.** Examples of simulated profiles with different roughness (Class A, B, C, and D).

movements are vertical displacements: ZsFR, ZsFL, ZsRR, ZsRL, and ZsAS). The quality of the optimization was assessed by a root mean square error, which represents the performance of the network, and a correlation coefficient R between the target data (simulation values) and the output data (i.e. ANN output values).

In this section, we show the results concerning the simulation of the Quarter Car and 5-DOF model. Regarding the Quarter Car model, a comparison between the basic configuration and the optimized configuration was carried out in order to highlight the improvement of the optimized configuration. Then, ANN was implemented in the model in order to predict the optimal suspension parameters and the same methodology was applied to the 5-DOF model.

The quality of the ANN prediction of the optimized parameters was assessed by a correlation coefficient R between the target data and the output data for training, validation and testing, and the root mean square error for the best validation performance. Given the simplicity of the model, the best validation performance is achieved after five epochs with $R = 0.99$, as shown in Figure 11.

The performance of the whole ambulance active suspension system is tested under different road profiles based on simulation of the intended ANN control of the active suspension and compared with the passive suspension. As described above, five single exit networks are considered, these are then trained with the Modified Backward Propagation (MBP) algorithm which is known for its speed and simplicity of programming. Different structures are tested: (6-5-1); (6-7-1); (6-10-1); (6-12-1); (6-15-1); (6-18-1); (6-20-1) for each quality parameter. Where 6 are the input values, 1 is

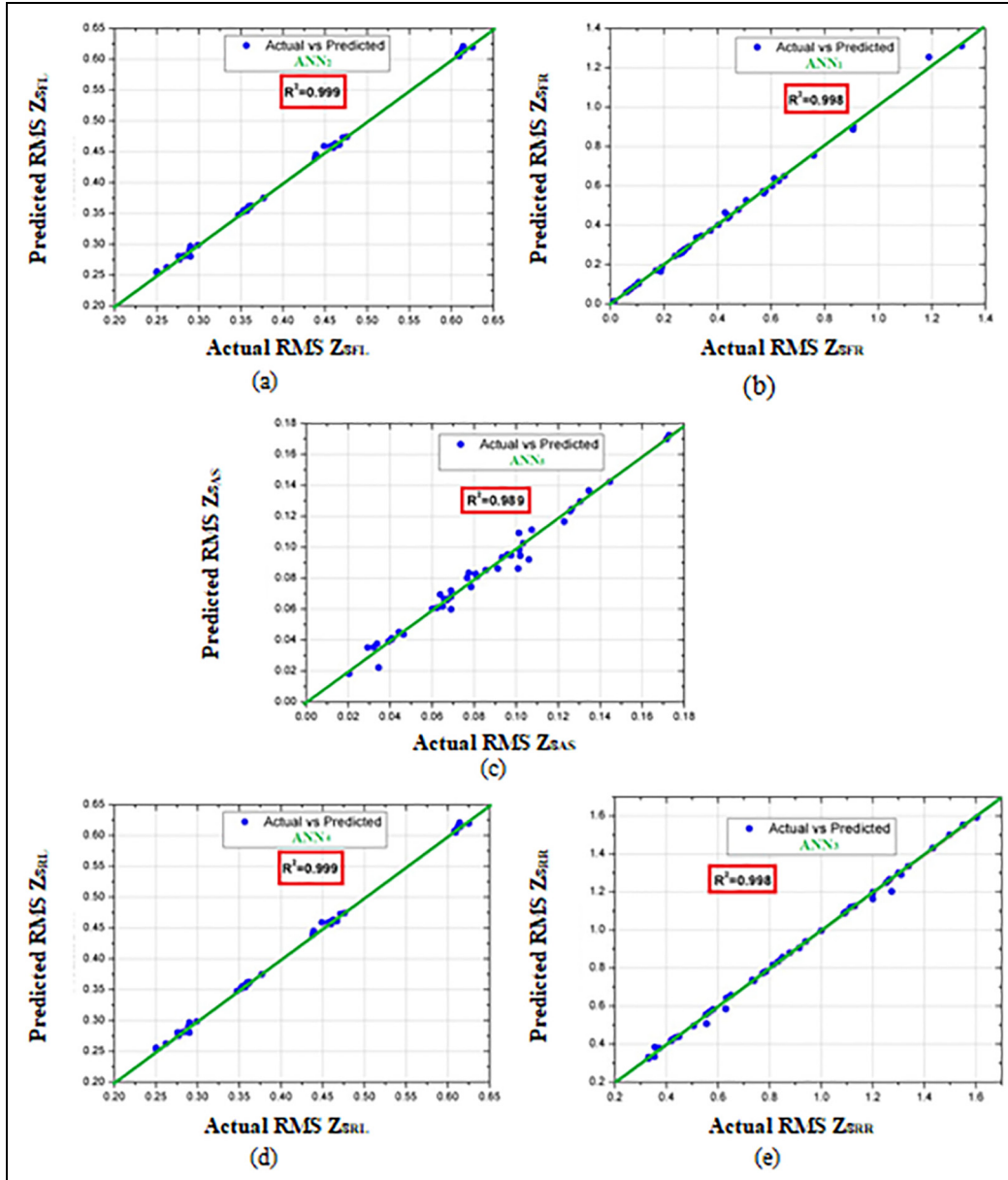


Figure 11. Regression curve between actual and predicted values of RMS sprung acceleration of: (a) the front left wheel Z_{sFL} model, (b) the front right wheel Z_{sFR} model, (c) the rear left wheel Z_{sRL} model, (d) the rear right wheel Z_{sRR} model, and (e) the ambulance stretcher Z_{sAS} model.

the correct output (target) values for a particular training data item and the number of hidden nodes, (5, 7, 10, 12, 15, 18, and 20) is arbitrary.

The linear relationship between predicted values and actual values (experimental) is shown in Figure 11 below. In statistics, Pearson's linear coefficient of determination, noted R^2 , is a measure of the quality of the prediction of a linear regression. We observe that the R^2 in the five quality parameters was between 0.989 and 0.999, indicating perfect ANN consistency. The scattered distribution of predicted values and predicted values with linear regression R^2 trends is shown in Figure 11.

In order to test and validate each model, the ANN, RMSE, AARE (Average Absolute Relative Error), AAE (Average Absolute Error), and R^2 indicators were used to compare the measured and estimated suspended

mass acceleration value (RMS Z_{sFL} , RMS Z_{sFR} , RMS Z_{sRL} , RMS Z_{sRR} and RMS Z_{sAS}).

Let us suppose that $(\ddot{Z}s)_{Pred}$ is the vector denoting values of N number of predictions. Also, $(\ddot{Z}s)_{Act}$ is a vector representing n number of true values. Then, the formula for mean squared error is given by:

$$MSE = \frac{1}{N} \sum_{i=1}^N ((\ddot{Z}s)_{Act} - (\ddot{Z}s)_{Pred})^2 \quad (11)$$

The RMSE was calculated according to equation (10):

$$RMSE = \sqrt{\frac{1}{N} \sum_{i=1}^N ((\ddot{Z}s)_{Act} - (\ddot{Z}s)_{Pred})^2} \quad (12)$$

Table 3. The MSE by predicting the five RMS responses by a 6-n-l.

Proposed network N of neurons in hidden layer	6-n-l ANN Model									
	RMS $Z_{s_{FL}}$		RMS $Z_{s_{FR}}$		RMS $Z_{s_{RL}}$		RMS $Z_{s_{RR}}$		RMS $Z_{s_{AS}}$	
	Train	Test	Train	Test	Train	Test	Train	Test	Train	Test
5	0.0041	0.001	4.1e-05	3.5e-05	0.0062	0.0457	1.2e-04	3.1e-04	3.8e-05	2.1e-05
7	0.0031	0.0014	3.2e-05	2.2e-05	0.0042	0.0068	4.1e-05	1.2e-04	2.6e-05	2.7e-05
10	0.0039	0.0061	2.6e-05	2.7e-05	0.0031	0.0075	4.7e-05	9.5e-05	1.5e-05	2.6e-05
12	2.7e-04	4.5e-04	1.1e-05	2.1e-05	1.5e-04	2.9e-05	2.8e-05	1.4e-05	5.1e-06	8.8e-06
15	9.6e-04	2.8e-04	1.5e-05	1.7e-05	1.9e-04	0.0046	2.1e-04	1.2e-04	4.1e-05	4.2e-05
18	8.1e-04	4.5e-04	2.7e-05	3.7e-05	9.6e-04	0.0045	1.2e-04	1.5e-04	1.5e-05	1.6e-05
20	5.8e-04	7.3e-04	1.3e-04	1.1e-4	5.1e-04	0.0056	1.3e-04	2.6e-04	3.6e-05	8.9e-06

Table 4. The MSE by predicting the five RMS responses by a 6-n-l.

Proposed network N of neurons in hidden layer	6-n-l ANN Model									
	RMS $Z_{s_{FL}}$		RMS $Z_{s_{FR}}$		RMS $Z_{s_{RL}}$		RMS $Z_{s_{RR}}$		RMS $Z_{s_{AS}}$	
	MRE	R ²	MRE	R ²	MRE	R ²	MRE	R ²	MRE	R ²
5	0.056	0.97	0.016	0.996	0.47	0.821	0.168	0.927	0.048	0.976
7	0.046	0.98	0.011	0.997	0.41	0.854	0.089	0.963	0.030	0.9
10	0.031	0.96	0.012	0.997	0.305	0.962	0.090	0.947	0.025	0.991
12	0.014	0.999	0.005	0.998	0.076	0.999	0.052	0.998	0.017	0.989
15	0.019	0.992	0.008	0.997	0.159	0.988	0.130	0.938	0.039	0.98
18	0.015	0.993	0.013	0.996	0.066	0.978	0.179	0.945	0.026	0.993
20	0.02	0.995	0.019	0.993	0.087	0.981	0.074	0.964	0.028	0.985

Then, the comparative precision between the experimental and predicted data was determined by examining their mean relative errors (MRE).^{38,39} The MRE gives an indication of the accuracy of the experimental data compared to the predicted data. MREs are defined with the following equation:

$$MRE = \frac{MSE}{(\ddot{Z}s)_{Act}} \quad (13)$$

The AAE and AARE according to equations (12) and (13) were calculated:

$$AAE = \frac{1}{N} \sum_{i=1}^N |(\ddot{Z}s)_{Act} - (\ddot{Z}s)_{Pred}| \quad (14)$$

$$AARE = 100 * AAE = \frac{100}{N} \sum_{i=1}^N |(\ddot{Z}s)_{Act} - (\ddot{Z}s)_{Pred}| \quad (15)$$

A comparison of the results for the different structures is shown in Tables 3 and 4. Regression analysis was used to assess the ability of the network to estimate different outputs in various ANN model architectures. The R^2 was used to measure the correlation between

the prediction of the formed network and the experimental data. The correlation coefficient (R) and determination coefficient (R^2) was calculated according to equations (16) and (17).⁴⁰

The regression coefficients R and R^2 are defined with the following equation:

$$R^2 = \frac{\sum_{i=1}^N ((\ddot{Z}s)_{Act} - \overline{(\ddot{Z}s)})^2 - \sum_{i=1}^N ((\ddot{Z}s)_{Act} - (\ddot{Z}s)_{Pred})^2}{\sum_{i=1}^N ((\ddot{Z}s)_{Act} - \overline{(\ddot{Z}s)})^2} \quad (16)$$

$$R = \sqrt{\frac{1 - \sum_{i=1}^N ((\ddot{Z}s)_{Act} - (\ddot{Z}s)_{Pred})^2}{\sum_{i=1}^N ((\ddot{Z}s)_{Act} - \overline{(\ddot{Z}s)})^2}} \quad (17)$$

Where, N is the number of data observations, $(\ddot{Z}s)_{Act}$ is the actual sprung mass acceleration, $(\ddot{Z}s)_{Pred}$ is the estimated value, and $\overline{(\ddot{Z}s)}$ is the experimental value.

RMSE provides information about the short-term performance of ANN models, as it allows a term-by-term comparison of the actual deviation between the

Table 5. The comparative analysis of performance index.

Performance index		Passive system ⁴¹	G.A. Active system ⁴¹	A.N.N Active system
Vertical acceleration of the stretcher centroid (m/s ²)	MAX	5.4344	2.8119	1.409
	RMS	1.9211	0.7818	0.7135
Pitch acceleration of the stretcher (rad/s ²)	MAX	1.0235	0.1489	
	RMS	0.3413	0.0512	
Dynamic displacement at the front of the stretcher (mm)	MAX	15.1	12.0	6.7
Dynamic displacement at the rear of the stretcher (mm)		22.0	18.5	
Front suspension dynamic displacement (mm)		28.397	22.629	18.4
Rear suspension dynamic displacement (mm)		32.719	27.940	22.3
Dynamic displacement of the front wheel (mm)		1.827	1.809	1.792
Dynamic displacement of the front wheel (mm)		2.401	2.374	2.358

calculated and measured suspended mass acceleration value. An RMSE value of zero would indicate that all output values calculated by the ANN fully match the corresponding measured suspended mass acceleration values. The closer the values of R^2 are to unity, the more linear the relationship between the estimated and measured models of suspended mass acceleration values. RMSE values close to zero and R^2 values close to 1 indicate that the ANN model provides accurate predictions. The RMSE coefficient is a measure of the accuracy and reliability of the calibration and test data sets.

By iteratively changing the number of neurons in the hidden layers, optimal network performance has been achieved. During the training procedure, the network developed with the least MRE and MSE and the highest correlation coefficient R^2 was selected. The best results against the objectives were identified by a weak MSE.

Table 3 gives the MSE rating of each model at the training and testing stages.

The 6-12-1 ANN model has the best capacity for all parameter outputs. It revealed the MSE of the lowest train for RMS of sprung acceleration of the front left wheel Z_{sFL} ($MSE-Z_{sFL} = 2.8 \cdot 10^{-4}$), RMS of sprung acceleration of the front right wheel Z_{sFR} ($MSE-Z_{sFR} = 1.1 \cdot 10^{-5}$), RMS of sprung acceleration of the rear left wheel Z_{sRL} ($MSE-Z_{sRL} = 1.5 \cdot 10^{-4}$), RMS of sprung acceleration of the rear right wheel Z_{sRR} ($MSE-Z_{sRR} = 2.9 \cdot 10^{-5}$) and RMS of sprung acceleration of the ambulance stretcher Z_{sAS} ($MSE-Z_{sFL} = 5.1 \cdot 10^{-6}$). The same interpretation can be observed for the value of the correlation coefficient (R^2) which is equal to 0.99 for sprung acceleration of the four wheels (RMS Z_{sFL} , RMS Z_{sFR} , RMS Z_{sRL} , and RMS Z_{sRR}) and 0.98 for the sprung acceleration of the ambulance stretcher (RMS Z_{sAS}). The 6-12-1 ANN model also showed excellent predictability with the least amount of error. All results showed an excellent in association between actual input parameters and expected output parameters. The generated ANN model can predict the quality parameters with the highest level of certainty for a new set of inputs addition, the mean relative error

(MRE) for the prediction of these outputs is 0.014, 0.005, 0.076, 0.052, and 0.017, respectively (Table 4).

Comparative analysis

In order to realize the rapid transport of the patient, the ambulance moves at high speed. In this article, we choose the condition of driving in a straight line at from 50 km/h (at about 14 m/s) to 110 km/h (at about 30 m/s), taking into account the white noise input of each class of road profile chosen in the simulation. In addition, we will compare our results found in this article with the work of Hou et al.⁴¹ from where we will be limited with this chosen speed of the ambulance.

In order to realize the rapid transport of the patient, the ambulance moves at high speed. In this comparative analysis, we choose the condition of driving in a straight line at 30 m/s (at about 110 km/h), considering the input of white noise from the road. The genetic algorithm was used in Hou et al.⁴¹ work to optimize the weighting matrix in the simulation model, so that we could perform the numerical simulation of the vibration isolation system of the two-dimensional stretcher. The results in the time domain and the comparison with our model based on neural networks are presented in Table 5. The parameters of two models, used in the articles, are very close to each other, hence the comparison has an approximate scientific significance of the efficiency of our controller based on the networks of artificial neurons.

It is important to note that in our model used we neglected the pitch acceleration of the stretcher and in the application of artificial neuron networks, we agreed to our work on the reduction of vertical acceleration of the stretcher centroid. This gives us a new perspective for our research in future articles.

Conclusion and scope for future work

Our goal in this research is to design an intelligent ambulance suspension system to transport the patient safely. The ideal suspension should independently absorb road shock quickly and so slowly return to its normal position. This behavior is difficult to attain

passively, since a versatile spring allows an excessive amount of movement and a tough spring causes discomfort to the passenger thanks to irregularities on the road.

The effects of acceleration on a patient being carried by ambulance are discussed in this work. The translational acceleration of the patient's complete body was estimated using a novel intelligent system controlled by five networks of artificial neurons, and the vehicle conducts five distinct moves (ANN1, ANN2, ANN3, ANN4, and ANN5). In step with previous work, the acceleration results obtained here are often detrimental to the physical integrity of patients transported within the ambulance, indicating the necessity to scale back vibrations within the ambulance stretcher. Vibrations on the patient's body can be lessened by installing an energetic suspension, controlled by artificial neural networks, between all of the wheels and the ambulance's body, or by installing a device under the stretcher. The simulation of the newly created system gave good prediction results to preserve patient transport using ANN techniques. The perspectives of this study might be a synthesis of a mechanism for reducing the consequences of vibrations within the translational and rotational movements of the ambulance stretcher.

Declaration of conflicting interests

The author(s) declared no potential conflicts of interest with respect to the research, authorship, and/or publication of this article.

Funding

The author(s) received no financial support for the research, authorship, and/or publication of this article.

ORCID iD

Anis Hamza  <https://orcid.org/0000-0003-4283-5236>

References

1. Hamza A, Ayadi S and Hadj-Taieb E. Propagation of strain waves in cylindrical helical springs. *J Vib Control* 2015; 21(10): 1914–1929.
2. Hamza A, Ayadi S and Hadj-Taieb E. Resonance phenomenon of strain waves in helical compression springs. *Mech Ind* 2013; 14: 253–265.
3. Hamza A, Ayadi S and Hadj-Taieb E. The natural frequencies of waves in helical springs. *Comptes Rendus Mécanique* 2013; 341: 672–686.
4. Hamza A and Ben Yahia N. Intelligent neural network control for active heavy truck suspension. In: Benamara A, Haddar M, Tarek B, et al. (eds) *Advances in mechanical engineering and mechanics, CoTuMe 2018, LNME*. Cham: Springer Science and Business Media LLC, 2019, pp.16–23.
5. Joshi OP, Jadhav TA, Pawar PR, et al. Investigating effect of road roughness and vehicle speed on the dynamic response of the seven degrees-of-freedom vehicle model by using artificial road profile. *Int J Curr Eng Technol* 2015; 5: 2596–2602.
6. Corum M, Basoglu C, Yakal S, et al. Effects of whole body vibration training on isokinetic muscular performance, pain, function, and quality of life in female patients with patellofemoral pain: a randomized controlled trial. *J Musculoskelet Neuronal Interact* 2018; 18: 473–484.
7. Sagawa K, Inooka H, Ino-oka E, et al. On an ambulance stretcher suspension concerned with the reduction of patient's blood pressure variation. *Proc IMechE, Part H: J Engineering in Medicine* 1997; 211: 199–208.
8. Henderson RJ and Raine JK. A two-degree-of-freedom ambulance stretcher suspension, part 2: simulation of system performance with capillary and orifice pneumatic damping. *Proc IMechE, Part D: J Automobile Engineering* 1998; 212: 227–240.
9. Sagawa K and Inooka H. Ride quality evaluation of an actively-controlled stretcher for an ambulance. *Proc IMechE, Part H: J Engineering in Medicine* 2002; 216: 247–256.
10. Cao D, Rakheja S and Su CY. Dynamic analyses of heavy vehicle with pitch-interconnected suspensions. *Int J Heavy Veh Syst* 2008; 15: 272–308.
11. Zhang N, Smith WA and Jeyakumaran J. Hydraulically interconnected vehicle suspension: background and modelling. *Veh Syst Dyn* 2010; 48: 17–40.
12. Xu XX, Wang M, Cui XD, et al. Simulation analysis and optimization design for vibration damping of stretchers on emergency ambulance. *J Vib Eng* 2009; 22: 352–356.
13. Pan GY and Zhang Y. Study on ambulance stretcher vibration isolation system. *Appl Mech Mater* 2012; 226–228: 324–327.
14. Yang M, Xu X and Su C. A study on vibration characteristics and stability of the ambulance nonlinear damping system. *Abstr Appl Anal* 2013; 2013: 1–12.
15. Yang M, Xu X, Su W, et al. The dynamic performance optimization for nonlinear vibration-reduction system of the tracked ambulance. *Proc IMechE, Part C: J Mechanical Engineering Science* 2015; 229: 2719–2729.
16. Prehn J, McEwen I, Jeffries L, et al. Decreasing sound and vibration during ground transport of infants with very low birth weight. *J Perinatol* 2015; 35: 110–114.
17. Chae HD and Choi SB. A new vibration isolation bed stage with magnetorheological dampers for ambulance vehicles. *Smart Mater Struct* 2015; 24: 017001.
18. Ding F, Zhang N, Liu J, et al. Dynamics analysis and design methodology of roll-resistant hydraulically interconnected suspensions for tri-axle straight trucks. *J Franklin Inst* 2016; 353: 4620–4651.
19. Yang W, Nong Z, Bangji Z, et al. Modeling and performance analysis of a vehicle with kinetic dynamic suspension system. *Proc IMechE, Part D: J Automobile Engineering* 2019; 233: 697–709.
20. Tan B, Wu Y, Zhang N, et al. Improvement of ride quality for patient lying in ambulance with a new hydro-pneumatic suspension. *Adv Mech Eng* 2019; 11: 2019.

21. The European Standard, EN 1789, Medical vehicles and their equipment – road ambulances, 2020.
22. The European Standard, EN 1865, Patient handling equipment used in road ambulances – part 2: power assisted stretcher, 2010.
23. International Organization for Standardization (IOS). Mechanical vibration and shock – evaluation of human exposure to whole-body vibration – part 5: method for evaluation of vibration containing multiple shocks. ISO 2631–5. Geneva, Switzerland: International Organization for Standardization, 2018.
24. Menon VA. Product development approach for a stabilized ambulance stretcher. Master's Thesis, Higher Engineering Institute of Porto, Porto, Portugal, 2018.
25. Kennedy J, Oakley C, Sumon S, et al. Impact of road humps on vehicles and their occupants, prepared for charging and local transport division, Report TRL614, 2004.
26. International Organization for Standardization. Mechanical vibration and shock – evaluation of human exposure to whole-body vibration. Geneva, Switzerland: International Organization for Standardization, 1997.
27. Eriksson J and Svensson L. Tuning for ride quality in autonomous vehicle. Master's Thesis, Uppsala University, Uppsala, Sweden, 2015.
28. Raemaekers A. Active vibration isolator design for ambulance patients. Master's thesis, Eindhoven University of Technology, Eindhoven, Holland, 2009.
29. British Standard Institution (BSI). Proposals for generalised road inputs to vehicles, BSI MEE/158/3/1, London, BSI 72/34562, 1972.
30. International Organization for Standardization. ISO 8608, mechanical vibration-road surface profiles-reporting of measured data. Geneva, Switzerland: International Organization for Standardization, 1995.
31. Demetriades D, Chan L, Cornwell E, et al. Paramedic vs private transportation of trauma patients: effect on outcome. *Arch Surg* 1996; 131: 133–138.
32. Johnson NJ, Carr BG, Salhi R, et al. Characteristics and outcomes of injured patients presenting by private vehicle in a state trauma system. *Am J Emerg Med* 2013; 31(2): 275–281.
33. The New Fiat Ducato: more technology, more efficiency, and more value. Fiatprofessionalpress.com. Archived from the original on 25 April 2014.
34. Griffin MJ. *Handbook of human vibration*. London: The University Southampton, Academic Press Limited, 1990.
35. Hamza A. Development of a model to assist the design of active mechanisms for suspension of heavy-duty trucks according to a multi-criteria approach. Doctoral Thesis, National School of Engineering of Tunis (ENSIT), University of Tunis, 2021.
36. Hamza A and Ben Yahia N. Heavy trucks with intelligent control of active suspension based on artificial neural networks. *Proc IMechE, Part I: J Systems and Control Engineering* 2021; 235: 952–969.
37. Abramov S, Mannan S and Durieux O. Semi-active suspension system simulation using Simulink. *Int J Eng Syst Modelling Simul* 2009; 1: 101–114.
38. Akricchi S, Abid S, Bouzaïen H, et al. SPIF quality prediction based on experimental study using neural networks approaches. *Mech Solids* 2020; 55: 138–151.
39. Akricchi S, Abbassi A, Abid S, et al. Roundness and positioning deviation prediction in single point incremental forming using deep learning approaches. *Adv Mech Eng* 2019; 11: 1–15.
40. Akricchi S, Abbassi A and Ben Yahia N. A new CAD-CAM approach using interacting features for incremental forming process. In: Benamara A, Haddar M, Tarek B, et al. (eds) *Advances in mechanical engineering and mechanics. CoTuMe 2018. Lecture notes in mechanical engineering*. Cham: Springer, 2019, pp.103–111.
41. Hou L, Liu S, Sun Q, et al. Optimal control of active ambulance stretcher suspension based on genetic algorithm. In: *2017 Chinese automation congress (CAC)*, Jinan, China, 20–22 October 2017, pp.6771–6776. New York: IEEE.